NJC

PAPER

View Article Online
View Journal | View Issue

Cite this: *New J. Chem.*, 2017, **41**, 12843

Probing the competition between acetate and 2,2′-bipyridine ligands to bind to d-block group 12 metals†

José Antônio do Nascimento Neto,[a] Cameron Capeletti da Silva,[a] Leandro Ribeiro,[a] Géssica Adriana Vasconcelos,[a] Boniek Gontijo Vaz,[a] Vinicius Sousa Ferreira,[a] Luiz Henrique Keng Queiroz Júnior,[a] Lauro June Queiroz Maia,[b] Ariel M. Sarotti[c] and Felipe T. Martins*[a]

Received 3rd July 2017,
Accepted 25th September 2017

DOI: 10.1039/c7nj02393f

rsc.li/njc

Herein, we were interested in probing the competition between 2,2′-bipyridine (2,2′-bipy) and acetate ligands in binding to Zn^{2+}, Cd^{2+} and Hg^{2+}. We have obtained eight new supramolecular architectures through tuning the proportion of these two ligands. On doubling the acetate availability compared to 2,2′-bipy, complexes with either Zn^{2+}, Cd^{2+} or Hg^{2+} were formed with one 2,2′-bipy and two acetate ligands coordinated to the metal center. One water molecule is also coordinated to Zn^{2+} and Cd^{2+} in these two complexes, which are reported here for the first time. One 2,2′-bipy is still coordinated to the three metal ions with an acetate excess of 10-times, but another trinuclear Zn^{2+} complex is formed with two 2,2′-bipy and six acetate ligands (1 : 3 2,2′-bipy : acetate stoichiometry). Upon setting an equimolar ratio of the ligands, the complex $[Zn(CH_3CO_2)(2,2'\text{-bipy})_2]^+$ is formed, while two 2,2′-bipy and two acetate ligands are coordinated to Cd^{2+}, giving rise to a $[Cd(CH_3CO_2)_2(2,2'\text{bipy})_2]$ complex. On doubling the 2,2′-bipy availability compared to acetate, the former does not coordinate to Zn^{2+} and Cd^{2+}, as observed in the acetate salt form of $[Zn(2,2'\text{-bipy})_3]^{2+}$ and in $[Cd(2,2'\text{-bipy})_3]^{2+}$. This last Cd^{2+} complex did not crystallize, revealing its unfavorable crystallization as an acetate salt form. However, under this last ligand ratio, the persistence of at least one coordinated acetate was observed in the Hg^{2+} complex with 2 : 1 2,2′-bipy : acetate stoichiometry. Furthermore, there is a cocrystallized 2,2′-bipy in the acetate salt form of $[Hg(CH_3CO_2)(2,2'\text{-bipy})_2]^+$, which is not able to win the competition with acetate for the third coordination site to Hg^{2+}. Even if the 2,2′-bipy amount is 10-times higher than that of acetate in the reaction batch, one acetate remains coordinated to Hg^{2+}. Our crystal form of $[Zn(CH_3CO_2)(2,2'\text{-bipy})_2]^+$ is strongly photoluminescent, with highly efficient emission centered at 356 nm (external and internal quantum yields of 14.2(1)% and 41.3(1)%), whose optical efficiency was rationalized on the basis of time-dependent DFT calculations.

Introduction

Coordination chemistry has been well developed in the past few decades.[1] Besides the interest in coordination compounds due to the possibility of the progress in basic structural chemistry,[2] they can have many desirable properties, such as in nonlinear optics and luminescence,[3–5] catalysis,[6] pharmaceuticals,[7,8] electronics[4,9] and others. The arrangements and structures of coordination complexes can be infinite because of the multiple valences and different coordination geometries of the metal center. Besides, there are an enormous amount of organic binders which can be used in the synthesis. Therefore, there are many types of supramolecular assemblies with different topological types, such as discrete molecules and dimers, chains, sheets, and three-dimensional networks.[10] The coordination structure can also be influenced by synthetic factors (such as temperature,[11,12] solvent system and reaction stoichiometry[13,14]) and packing (such as hydrogen bonds,[15] π–π stacking,[16] steric hindrance from organic ligands and lattice counterions[16c,17]) aspects, unveiling the difficulty in obtaining a structurally designed complex.

Among all possible strategies for synthesis, the stoichiometry of metal ions in solution has a critical role in the self-assembled

[a] *Instituto de Química, Universidade Federal de Goiás, Goiânia, PO Box 131, GO, 74690-900, Brazil. E-mail: felipe@ufg.br*
[b] *Instituto de Física, Universidade Federal de Goiás, Campus Samambaia, Goiânia, CP 131, GO, 74001-970, Brazil*
[c] *Instituto de Química Rosario (IQUIR), Universidad Nacional de Rosario-CONICET, Suipacha 531, S2002LRK Rosario, Argentina*

† Electronic supplementary information (ESI) available: PDF file comprising Tables S1–S6 and Fig. S1–S26. CCDC 1522495, 1522500, 1522502, 1522503, 1538392, 1538395–1538397. For ESI and crystallographic data in CIF or other electronic format see DOI: 10.1039/c7nj02393f

construction. The use of different proportions of stoichiometry can lead to the formation of completely different structures, because the number of possible binding sites is influenced by the number of molecules available to coordinate to the metal ion.[18]

In this work, we present new structures synthesized from metals of group 12: Zn^{2+}, Cd^{2+} and Hg^{2+} with the ligands acetate and 2,2′-bipyridine (2,2′-bipy). The former has been extensively used in the construction of metal–organic complexes due to its bidentate coordination mode associated with packing functionalities, such as versatile non-classical hydrogen bonding donor moieties and π-clouds that are able to establish π–π stacking interactions promptly, which means the possibility to control the geometry and connectivity of the generated coordination polymers.[19] More precisely, herein, we were interested in probing the competition between 2,2′-bipy and acetate ligands to bind to Zn^{2+}, Cd^{2+} and Hg^{2+}. Coordination complexes of these d-block metals were already reported,[16,20–25] but no systematic investigation of the role of the ligand ratio in the complex formation and crystal assembly is available. With our ongoing research on novel functional metal–organic compounds, we have obtained eight new supramolecular architectures of d-block group 12 metals through tuning the 2,2′-bipy : acetate ratio in the synthesis. In addition, two of them are made up of new molecular entities. Such a trivial synthetic approach has increased both molecular and structural diversity in the d-block group 12 metal complexes with these two common ligands, providing a new photoluminescent crystal form of high quantum efficiency. Therefore, this straightforward and practical strategy based on the ligand ratio range has been successfully employed here as a source of new complexes and crystal forms possessing the desired optical properties, which can motivate its application to other ligands and metal ions.

Experimental

All reagents were obtained from commercial sources and were used without further purification. In order to assess the competition between 2,2′-bipy and acetate ligands we carried out a crystallization screening with the stoichiometric ratio between them ranging from 1 : 10 to 10 : 1. All reactions were performed at room temperature by directly mixing the reagents in solution. Glass crystallizers containing the mixtures were then allowed to evaporate at room temperature and, after one week, crystals could be isolated from the mother solution. The crystallization batches that yielded new crystal forms of complexes comprising 2,2′-bipy and acetate ligands will be described in sequence (see Fig. 1). Moreover, unit cell determination was performed for crystalline products obtained from initial ligand ratios other than those described in sequence, assigning, together with high resolution mass spectrometry (HRMS), which complex was obtained from each starting ligand ratio (Fig. 1).

Synthesis and crystallization

$[Zn_3(CH_3CO_2)_6(2,2'\text{-bipy})_2]$ (1A). An ethanolic solution (5 mL) of 2,2′-bipy (0.10 mmol, 15.6 mg) was mixed together with an aqueous solution of $Zn(CH_3CO_2)_2{\cdot}2H_2O$ (0.50 mmol, 109.8 mg).

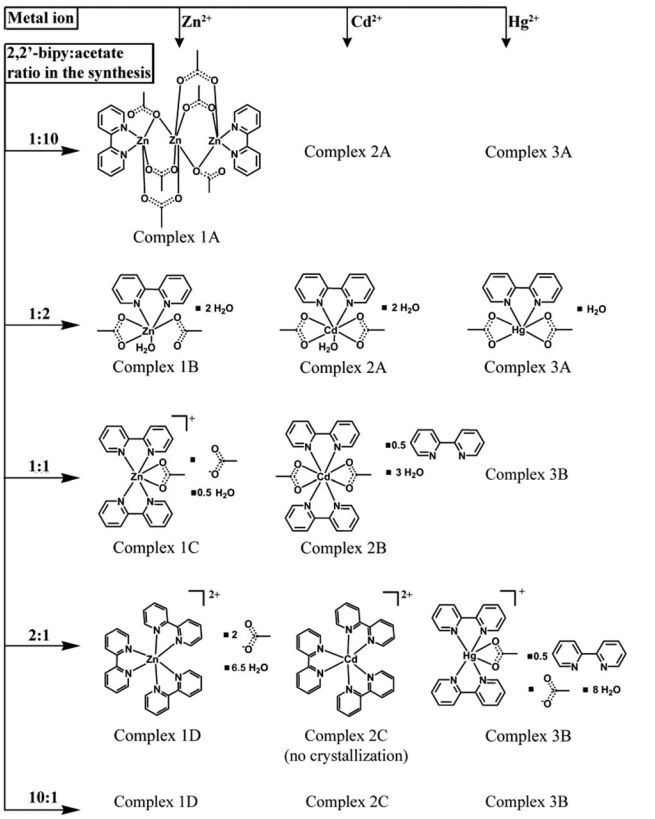

Fig. 1 General scheme of the preparation of the coordination complexes. Chemical diagrams are shown in the synthetic batches from which single crystals were isolated for structure determination.

$[Zn(CH_3CO_2)_2(2,2'\text{-bipy})(H_2O)]$ (1B), $[Cd(CH_3CO_2)_2(2,2'\text{-bipy})(H_2O)]$ (2A) and $[Hg(CH_3CO_2)_2(2,2'\text{-bipy})]$ (3A). A solution of 2,2′-bipy (0.10 mmol, 15.6 mg) in methanol was added to an aqueous solution of $Zn(CH_3CO_2)_2{\cdot}2H_2O$ (0.10 mmol, 21.9 mg). Compounds **2A** and **3A** were prepared similar to **1B**, although $Cd(CH_3CO_2)_2{\cdot}2H_2O$ (0.10 mmol, 26.7 mg) and $Hg(CH_3CO_2)_2$ (0.10 mmol, 31.8 mg) were used instead.

$[Zn(CH_3CO_2)(2,2'\text{-bipy})_2]^+$ (1C) and $[Cd(CH_3CO_2)_2(2,2'\text{-bipy})_2]$ (2B). Compound **1C** was prepared similarly to compound **1B**, but, in this case, an amount of 2,2′-bipy (0.10 mmol, 15.6 mg) and $Zn(CH_3CO_2)_2{\cdot}2H_2O$ (0.05 mmol, 11.0 mg) was used. To prepare complex **2B**, $Cd(CH_3CO_2)_2{\cdot}2H_2O$ (0.05 mmol, 13.3 mg) was used rather than the zinc acetate salt.

$[Zn(2,2'\text{-bipy})_3]^{2+}$ (1D) and $[Hg(CH_3CO_2)(2,2'\text{-bipy})_2]^+$ (3B). Compound **1D** was prepared by adding a methanol solution of 2,2′-bipy (0.32 mmol, 50 mg) to an aqueous solution of $Zn(CH_3CO_2)_2{\cdot}2H_2O$ (0.016 mmol, 3.5 mg). Compound **3B** was synthesized using the same ligand ratio for **1D**, however $Hg(CH_3CO_2)_2$ (0.016 mmol, 5.0 mg) was used instead.

Structure determination of compounds

All reflection data were obtained on a Bruker-AXS Kappa Duo diffractometer with an APEX II CCD detector with a monochromated X-ray beam (Mo Kα radiation = 0.71073 Å). For the data frame integration, the SAINT and SADABS programs were used.[26] Structures were solved by direct methods of phase

retrieval with SHELXS-2014,[27] and the refinement was performed by full-matrix least squares on F^2 with SHELXL-2014.[27] All non-hydrogen atoms were refined with free anisotropic displacement parameters, while the hydrogen atoms had their displacement parameters fixed and set to isotropic. Their isotropic thermal parameters were set to 1.2 times the U_{eq} of the bonded sp^2 carbon or nitrogen or 1.5 times the U_{eq} of the bonded sp^3 carbon or oxygen. The hydrogen positions were calculated according to both intramolecular and intermolecular requirements and were constrained following a riding model. In the structure of complex **1A**, the zinc atom Zn2 lies on a crystallographic inversion centre at the (0.5, 0.5, 0.5) position. Therefore, its occupancy factor was set to 50%. In the crystal structure of complex **1C**, there is one water molecule whose atomic occupancy factors were restrained to 50%. Furthermore, there is also one acetate counterion disordered over two site sets of 50% occupancy, which balances the charge within this crystal lattice. The structure analysis and preparation of artwork were performed with MERCURY[28] and ORTEP-3[29] within the WinGX[29] software package. The details of the single crystal X-ray diffraction experiments are presented in Table S1 in the ESI.†

Mass spectrometry, nuclear magnetic resonance (NMR), infrared (IR) and UV spectroscopy

The positive ion high-resolution mass spectra were obtained on a Orbitrap Q-Exactive mass spectrometer (Thermo Scientific, Bremen, Germany) equipped with a heated electrospray ion source. The parameters used were: spray voltage 3 kV; capillary temperature 250 °C; Fourier transform MS resolution 140 000; S-Lens Level 50; sheath gas 10 (arbitrary units). The mass spectra were recorded in continuous monitoring mode with a mass range of 200–1000. The crystalline products from all synthetic 2,2′-bipy : acetate ratios (Fig. 1) were dissolved in methanol to a concentration of 100 ng mL^{-1} using methanol, without the addition of a base or an acid. The resulting solution was analyzed by direct infusion through a syringe pump (Hamilton 1750RN) at a flow rate of 3 μL min^{-1}. The data were evaluated using the XCALIBUR software 2.7 SP1 (Thermo Scientific, Bremen, Germany). The ^1H and ^{13}C NMR experiments were performed at 298 K on a Bruker Avance III 500 spectrometer, operating at 500.13 MHz for ^1H and 125.03 MHz for ^{13}C, equipped with a 5 mm *z*-gradient TBI probe (^1H, ^{13}C and XBB), using methanol-d_4 (500 μL) to prepare a solution with 1 mg of each complex. Transmission infrared spectra were recorded using a Spectrum 400FT-IR/FT-FIR spectrometer (PerkinElmer®). Samples were analyzed with KBr pellets (200 mg of KBr and 1 mg of each complex). Each FT-IR spectrum was averaged on 16 acquisitions at a spectral resolution of 4 cm^{-1}. UV-vis spectra were recorded in water solution at room temperature using a PerkinElmer model Lambda 45 – UV/VIS spectrophotometer in the 220 to 800 nm range with a fixed resolution slit of 2.0 nm. No absorption bands were observed in the visible region.

Photoluminescence (PL) excitation and emission measurements

PL excitation and emission spectra of the powdered crystals were acquired using a double monochromator and a Hamamatsu photomultiplier tube as a detector (Fluorolog FL3-221 from Horiba Jobin-Yvon), under excitation from a Xe arc lamp delivering a potency of 450 W. The used bandpass was 1.0 nm with a record step of 1.0 nm.

Theoretical calculations

In order to rationalize the photoluminescence observed for complexes **1C** and **2B**, we performed density functional theory (DFT) calculations.[30,31] The hybrid functional B3LYP[32,33] was used coupled with the 6-31G* basis set for H, C, O and N atoms, and the Los Alamos effective core potential plus double zeta (LANLDZ)[34] basis set for Cd and Zn atoms. The geometries of **1C** and **2B** were extracted from their crystal structures determined in this work, and the coordinates of all hydrogen atoms were optimized while freezing the internal coordinates of all the remaining heavy atoms. Further FMO and TD-DFT calculations were next carried out at the same level of theory using the partially optimized geometries as inputs. Similar calculations were also conducted using the fully optimized geometries (with no constraints) at the same level of theory. Frequency calculations were performed for the fully optimized geometries, which were found to be similar to the corresponding partially optimized ones, to determine the nature of the located stationary point. In all cases, positive definite Hessian matrices were found. All calculations were performed with the Gaussian 09 program package.[35]

Results and discussion

The role of the ligand ratio in synthesis

In this study, eight new crystal forms (Table S1, ESI†), two of which are composed of new coordination complexes, were obtained using 2,2′-bipy and acetate as ligands and metals from d-block group 12. Their labeling scheme was denoted with numbers **1**, **2** or **3** for Zn^{2+}, Cd^{2+} or Hg^{2+} followed by a capital letter ordered according to increasing number of coordinated 2,2′-bipy (Fig. 2). By doubling the acetate availability compared to 2,2′-bipy, three coordination complexes of either Zn^{2+} (**1B**), Cd^{2+} (**2A**) or Hg^{2+} (**3A**) with 2 : 1 2,2′-bipy : acetate stoichiometry were prepared. Complexes **1B** and **2A** also have one coordinated water molecule and they were not known thus far. Complexes **1A**, **2B** and **3A** had their crystal structures elucidated for the first time here,[16,22,24] while complexes **1C**, **1D** and **3B** were obtained in crystal forms different from those already reported in the literature.[20,21,25]

The persistence of at least one coordinated 2,2′-bipy or one acetate was observed even with either a 1 : 10 or 10 : 1 2,2′-bipy : acetate ratio, respectively. A trinuclear Zn^{2+} complex with 1 : 3 2,2′-bipy : acetate stoichiometry (**1A**) was obtained under such acetate excess. On the other hand, an acetate salt form of the Hg^{2+} complex with 2 : 1 2,2′-bipy : acetate stoichiometry (**3B**) was isolated in the presence of excess of 2,2′-bipy. In this last structure, one 2,2′-bipy molecule is cocrystallized in the lattice as it is present in excess, even though it is not able to substitute for the persistent coordinated acetate.

If a 2,2′-bipy excess is used, the Zn^{2+} and Cd^{2+} behaviors did not match that of Hg^{2+}. A synthetic 2 : 1 2,2′-bipy : acetate ratio

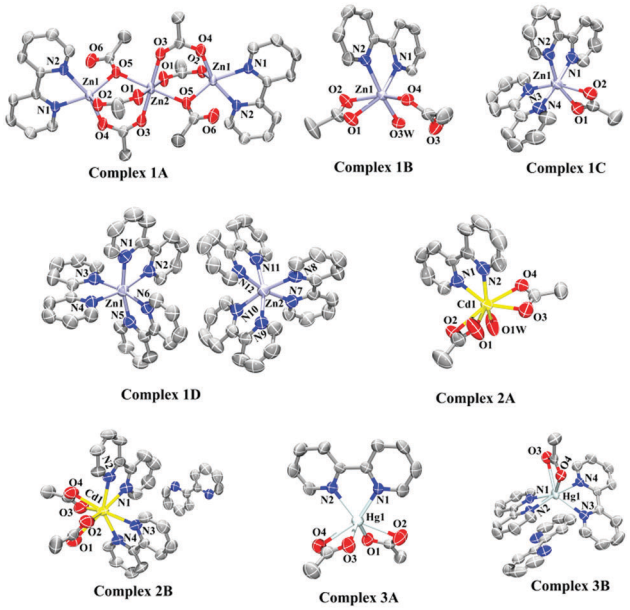

Fig. 2 ORTEP view of coordination complexes reported here shown with 50% probability level ellipsoids. Hydrogen atoms, crystallizing water and counter-ion species have been omitted for clarity. Only coordinated atoms were labeled.

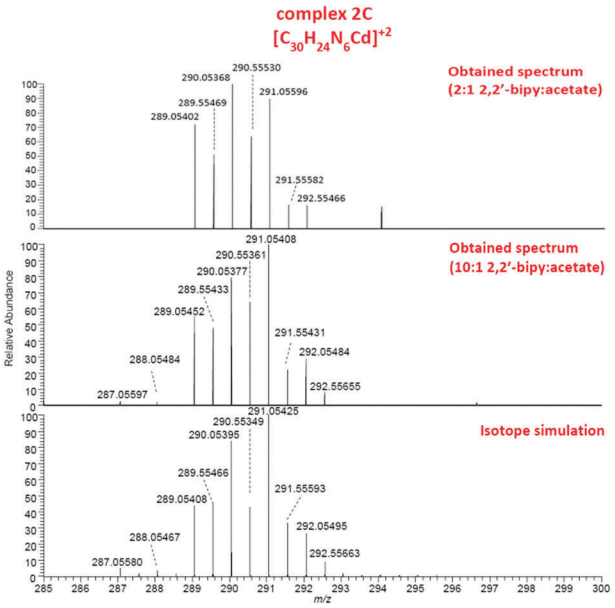

Fig. 3 ESI(+)-orbitrap mass spectrum of complex **2C**.

is already enough to unbind all acetate ligands. With this ratio and also using a larger 2,2′-bipy excess, an acetate salt form of the Zn^{2+} complex with three 2,2′-bipy ligands (**1D**) is formed. Such a Cd^{2+} complex with three 2,2′-bipy ligands (**2C**) is also obtained from both 2 : 1 and 10 : 1 2,2′-bipy : acetate ratios. However, **2C** did not crystallize as an acetate salt form, which indicates the role of the counterion in its crystal assembly. The perchlorate salt monohydrate of complex **2C** was already determined by a single crystal X-ray diffraction technique.[23] Herein, however, **2C** was identified by HRMS in methanol solutions prepared with non-crystalline products obtained from both initial 2 : 1 and 10 : 1 2,2′-bipy : acetate ratios (Fig. 3). The formation of a crystalline acetate salt was unfavorable for **2C**, different from that in the presence of perchlorate counterions.

With an equimolar ligand proportion, a new highly efficient photoluminescent crystal form of the known Zn^{2+} complex with 2 : 1 2,2′-bipy : acetate stoichiometry (**1C**) was obtained. Equimolar stoichiometry of ligands was observed only in another Cd^{2+} complex (**2B**), synthesized from the same equimolar ligand ratio. This solid state material also presented significant photoluminescence properties (see below). Based on all products from different starting ligand ratios, it was possible to conclude that the increase in sensibility was due to the changes in the proportion of these ligands from Hg^{2+} to Zn^{2+}.

A summary of the starting ligand ratios used to obtain each complex is shown in Fig. 1. All products obtained from each initial ligand ratio, crystalline or not, were characterized in methanol solution by HRMS (Fig. 3 and Fig. S1–S7, ESI†) and the identity of all of them (except **1A**) was in agreement with that found from single crystal structure determination and unit cell screenings (except for **2C** which was not crystalline).

In addition, all complexes were characterized by NMR (^{1}H and ^{13}C, Fig. S8–S16, ESI†), IR (Fig. S17, ESI†) and UV spectroscopy techniques (Fig. S18–S20, ESI†). All spectral assignments can be found in the ESI† in the corresponding figure caption and are in agreement with the structures determined crystallographically (or by HRMS in the case of **2C**), besides showing their bulky purity.

Crystal structures with Zn^{2+}

1A: $[Zn_3(CH_3CO_2)_6(2,2'\text{-bipy})_2]$. The crystal structure of **1A** was found to be similar to those already reported in the literature as a trinuclear complex with manganese ions, and also as heterometallic complexes.[16] The crystal structure of complex **1A** was solved in the $P\bar{1}$ space group of the triclinic crystal system. Its unit cell is composed of a trinuclear complex made up of three Zn^{2+} ions, two 2,2′-bipy molecules and six acetate anions. The peripheral Zn^{2+} cations (Zn1) are related by inversion symmetry and therefore, have the same coordination geometry, while the central metal (Zn2) lies on an inversion center at the (0.5, 0.5, 0.5) position. Thus, in this trinuclear complex with the general formula $[Zn_3(CH_3CO_2)_6(2,2'\text{-bipy})_2]$, Zn1 and Zn2 have different coordination environments and adopt different coordination geometries. Zn1 is five-coordinated in a distorted trigonal bipyramidal geometry, with two 2,2′-bipy nitrogen atoms (N1 and N2) and one oxygen (O4) of an acetate anion forming the basal plane, while the oxygens O2 and O5 of two different acetate ligands are in the axial positions. Meanwhile, Zn2 is six-coordinated and assumes an octahedral geometry with the surrounding (ZnO_6) being defined by oxygen atoms from the six acetate anions. Coordination angles and lengths for **1A** are summarized in Table S2 (ESI†) and all other crystal forms are elucidated here. The geometry of hydrogen bonds for this complex and all others is also presented in the ESI† (Table S3).

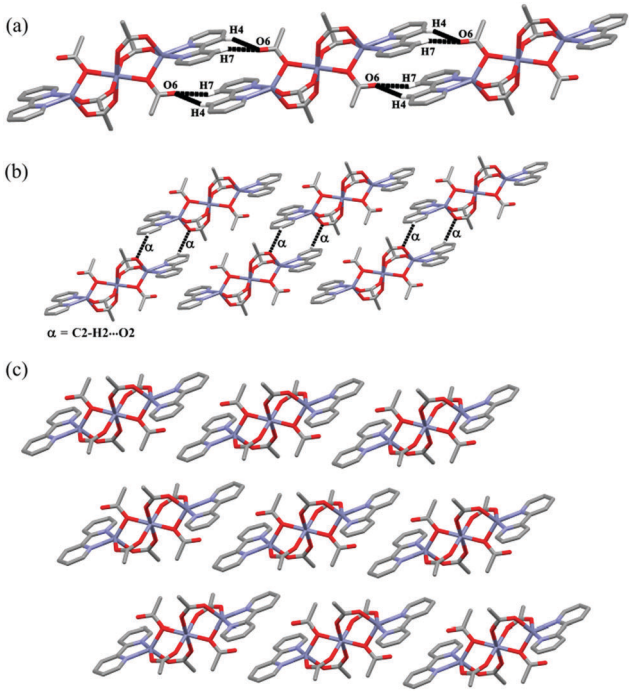

Fig. 4 (a) Chain made up of $[Zn_3(CH_3CO_2)_6(2,2'\text{-bipy})_2]$ units assembled by C–H···O interactions. (b) Two neighboring chains interlinked by C2–H2···O2 hydrogen bonds. Only the hydrogen atoms involved in intermolecular interactions are exhibited in both panels. (c) An overall packing piece of **1A**.

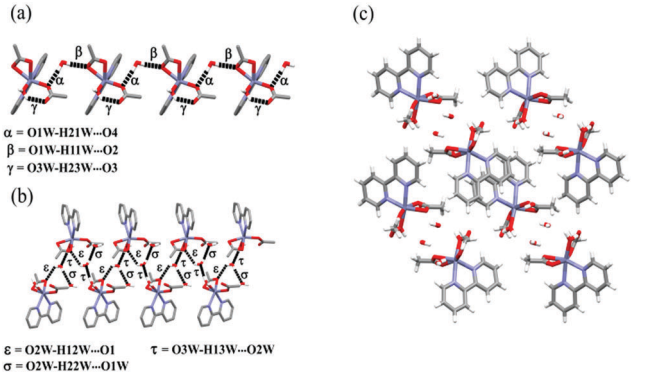

Fig. 5 (a) Infinite chain consisting of **1B** units and water. (b) Lattice water O2W connecting two chains shown in (a). (c) Packing of complex **1B** onto the *ac* plane.

Concerning the packing, non-classical hydrogen bonds C–H···O are responsible for assembling infinite chains made up of $[Zn_3(CH_3CO_2)_6(2,2'\text{-bipy})_2]$ units through the hydrogen atoms (H4 and H7) of the 2,2′-bipy ligand and the carboxylate-oxygen O6 of the monodentate acetate. In addition, different chains are interlinked by C–H···O contacts, generating a layered structure (Fig. 4).

The dihydrate form of 1B: $[Zn(CH_3CO_2)_2(2,2'\text{-bipy})(H_2O)]\cdot(H_2O)_2$. The crystal structure of **1B** was solved in the monoclinic space group *C*2/*c*, with one complex and two crystallizing water molecules in the asymmetric unit. The complex molecule $[Zn(CH_3CO_2)_2(2,2'\text{-bipy})(H_2O)]$ consists of one zinc atom coordinated by one water molecule, two bidentate ligands (one 2,2′-bipy and one acetate), and one monodentate acetate. Such non-coordinated acetate oxygen is intramolecularly bonded to water in complex **1B** (Fig. 5a) by a hydrogen bond. This interaction introduces a distortion in the octahedral coordination geometry. In such a geometry, three oxygens from two acetate ligands and one 2,2′-bipy nitrogen form the basal plane [root mean square deviation (RMSD) from the least-square plane of 0.143 Å for O1, O2, O4 and N1 atoms], while the other nitrogen (N2) and water oxygen (O3W) are at the apices of the octahedra. The 2,2′-bipy ligand is almost perpendicular to each acetate. The angles between their mean planes are 72.89°(12) and 87.09°(12).

The water molecules play a major role in the crystal packing of complex **1B**. Chains comprising **1B** molecules intercalated with lattice water ones are formed (Fig. 5a). Water O1W is responsible for keeping the units of **1B** together through the donation of two hydrogen bonds to the oxygens O2 and O4 of the acetate ligands. Besides, O1W is also a hydrogen bonding acceptor from water O2W by means of the O2W–H22W···O1W interaction. The water bearing O2W links two chains of complex **1B** by playing a dual role as a hydrogen bonding acceptor and a donor from the coordinated water and to the oxygen O1 of the bidentate acetate anion, respectively (Fig. 5b). Furthermore, the chains connected by the nearly described hydrogen bonding pattern are responsible for assembling sheets, wherein hydrophobic groups are oriented to opposite sides relative to the hydrophilic ones (Fig. 5c).

The acetate salt hemihydrate of 1C: $[Zn(CH_3CO_2)(2,2'\text{-bipy})_2]\cdot(CH_3CO_2)\cdot(H_2O)_{0.5}$. The crystal structure was solved in the triclinic space group $P\bar{1}$ and is composed of a discrete motif made up of two 2,2′-bipy, one acetate and one Zn^{2+}. The crystal structure of this complex has been previously elucidated as a hexafluorophosphate monohydrate[20a] and a perchlorate monohydrate.[20c,d] Besides one unit of the $[Zn(CH_3CO_2)(2,2'\text{-bipy})_2]^+$ complex, there is also one water molecule in the asymmetric unit and two acetate counterions. These last three species are in 50% occupancy sites and are lodged into hydrophilic channels. In complex **1C**, Zn^{2+} is coordinated to the four nitrogen atoms from two 2,2′-bipy and two oxygen atoms from acetate. Its coordination fashion and therefore the whole molecule resembles those reported previously for its other salt forms,[20] which can be observed in the low RMSD values calculated through the coordinated atoms and Zn^{2+} (Fig. 6). The two 2,2′-bipy ligands are almost perpendicular, as occurs in other crystal forms of this complex (hexafluorophosphate monohydrate and dicyanamide salts, and tetracyanoquinodimethane solvate respectively),[20a,b,e] while in perchlorate salts[20c,d] there are smaller angles (64.792(10)°) and (65.863 (67)°) between the 2,2′-bipy mean planes as can be seen in the table of Fig. 6.

It is important to observe the chain formation through non-classical C–H···O hydrogen bonding between 2,2′-bipy and acetate ligands (Fig. 7a). Such chains are also stabilized by π···π interactions between the aromatic rings from neighboring species of **1C**. To assemble this crystal structure, the chains are also packed on top of one another through C–H···π contacts between the methyl moiety of the acetate ligands and

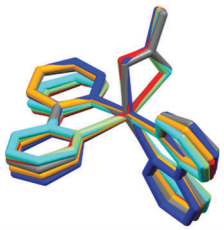

Crystal Form	Mean Zn-O values/Å	Mean Zn-N values/Å	RMSD values (Å) of molecule overlay for 1C found in different salt forms*	Dihedral angle between the least-squares planes through the two 2,2′-bipy ligands / degree#
$[Zn(CH_3CO_2)(bipy)_2](OH)\cdot(H_2O)_n$ &	2.212(7)	2.128(7)	——	74.727(13)
$[Zn(CH_3CO_2)(bipy)_2]PF_6\cdot(H_2O)$[20a]	2.198(3)	2.127(3)	0.0584	71.184(66)
$[Zn(CH_3CO_2)(bipy)_2][Mn(dca)_3(H_2O)$[20b]	2.233(1)	2.120(2)	0.0824	72.699(24)
$[Zn(CH_3CO_2)(bipy)_2]ClO_4\cdot(H_2O)$[20c]	2.200(4)	2.126(5)	0.0845	64.792(10)
$[Zn(CH_3CO_2)(bipy)_2]ClO_4\cdot(H_2O)$[20d]	2.181(3)	2.113(3)	0.0989	65.863(67)
$[Zn(CH_3CO_2)(bipy)_2]_2\cdot(TCNQ)\cdot(CH_3OH)$[20e]	2.167(3)	2.133(3)	0.1100	84.731(58)

& Reported in this work.
*The root mean square deviation (RMSD) were calculated through the coordinated atoms and metal ion.
The plane was calculated through the non-hydrogen atoms of 2,2′-bipy ligands.

Fig. 6 Molecular overlay for **1C** found in different salt forms.

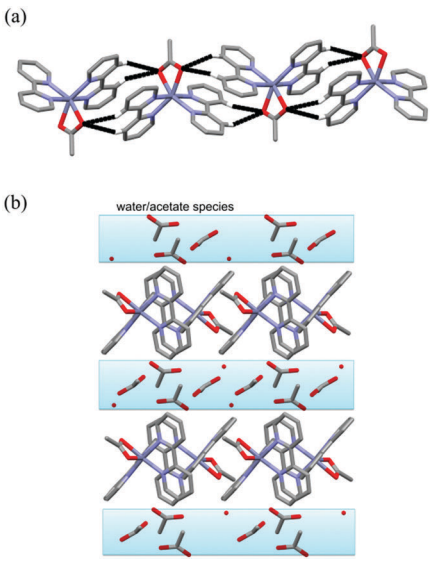

Fig. 7 (a) Chain composed of **1C** units held together through non-classical hydrogen bonding (C–H···O). Only hydrogen atoms involved in the intermolecular interactions are shown. (b) Layered structure intercalating water/acetate species and molecules of complex **1C**. The channels filled with water and acetates are highlighted in cyan.

2,2′-bipy molecules. Finally, water molecules and non-coordinated acetate counterions are engaged in the crystal packing, since they form channels between the chains of **1C** giving rise to a sandwich-like layered structure intercalating water/$CH_3CO_2^-$ species and molecules of the complex (Fig. 7b).

The acetate salt 6.5-hydrate of 1D: $[Zn(2,2'\text{-bipy})_3]\cdot(CH_3CO_2)_2\cdot(H_2O)_{6.5}$. The crystal structure of complex **1D** was already solved in hexafluorophosphate, perchlorate, sulfate and chromate salt forms, but not as an acetate salt.[21] Herein, its acetate salt is crystallized in the monoclinic space group $P2_1/c$. The asymmetric unit of the structure comprises two independent cationic complexes **1D**, four acetate anions and thirteen water molecules. In this crystal structure there are two different Zn^{2+} ions where both of them are six-coordinated with a distorted octahedral geometry (the RMSD values for Zn1 and Zn2 are 0.291 Å for the basal plane formed by N2, N3, N4 and N6 atoms, and 0.292 Å for the basal plane made up of N7, N8, N10 and N12 atoms, respectively) with their surrounding being defined by ZnN_6. The 2,2′-bipy molecules present in both cationic complexes are almost orthogonal to each other, with angles between their mean planes ranging from 81.44(13)° to 87.50(11)°.

Similar to that observed in complex **1C**, there is also the formation of channels within the crystal structure of **1D** (Fig. 8). These channels are filled with acetate anions and crystallizing water molecules. In complex **1D**, the water molecules and the acetate anions are engaged in a complex hydrogen bonding network giving rise to a hydrophilic layer alternated with a hydrophobic one built up of complex **1D** molecules.

Crystal structures with Cd^{2+}

The dihydrate of 2A: $[Cd(CH_3CO_2)_2(2,2'\text{-bipy})(H_2O)]\cdot(H_2O)_2$. Complex **2A** was prepared similarly to complex **1B**, although cadmium acetate dihydrate was used instead of the corresponding zinc salt. The same 1 : 2 2,2′-bipy : acetate ratio was used for their synthesis as mentioned earlier. This compound resembles the complex **1B** structure, with one 2,2′-bipy and two acetate ligands being present besides one coordinated water. In fact, neutral complex **2A** is very similar to complex **1B**, differing only in the coordination number around the metal center. In **1B**, one of the two acetate ligands is monodentate rather than bidentate as occurs with both acetate ligands of **2A** (Fig. 2). This similarity can also be viewed in Fig. 9, a molecular superimposition of complexes **2A** and **1B** (RMSD of 0.189 Å) through the metal ions, nitrogen atoms and carboxylate-oxygens of the bidentate acetate common to **2A** and **1B**.

Similar to the Zn^{2+} analog reported here, the crystal structure of **2A** was solved in the monoclinic space group $C2/c$. The complex

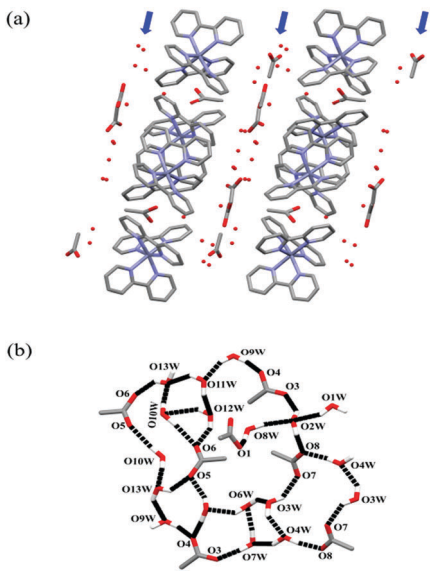

Fig. 8 (a) Channels (blue arrows) filled with water and acetate species are intercalated by layers made up of **1D**. (b) Water and acetate anions engaged in the hydrogen bonding network of the channels.

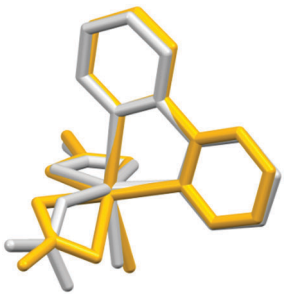

Fig. 9 Molecular overlay of complex molecules of **2A** (yellow) and **1B** (light gray).

molecule **2A** consists of one Cd^{2+} coordinated with one water molecule and three bidentate ligands (one 2,2′-bipy and two acetate anions). Its seven-coordinated geometry can be described as a distorted pentagonal bipyramid, in which the four acetate oxygens (O1, O2, O3 and O4) and one 2,2′-bipy nitrogen (N1) form a distorted basal plane (RMSD of the five fitted atoms is 0.796 Å), while another ligand nitrogen and water oxygen are at the axial positions. Each acetate ligand is almost orthogonal to the 2,2′-bipy mean plane, with angles between their mean planes measuring 72.0(4)° and 78.5(3)°.

Despite their molecular similarity, complexes **1B** and **2A** differ in their crystal packing. In **2A**, hydrogen bonds O1W–H11W···O2 and O1W–H21W···O4 assemble infinite chains constructed only with **2A** units (Fig. 10a), while non-coordinated water molecules have intercalated complex molecules of **1B** into its chains (Fig. 5a). Furthermore, non-coordinated crystallographically independent water molecules are responsible for contacting the chains of **2A** (Fig. 10b and c).

The 2,2′-bipy 0.5-cocrystal trihydrate of 2B: $[Cd(CH_3CO_2)_2(2,2'\text{-bipy})_2]\cdot(2,2'\text{-bipy})_{0.5}\cdot(H_2O)_3$. The structure of complex **2B** was solved in the triclinic space group $P\bar{1}$, with one complex unit, three crystallizing water molecules and half of a 2,2′-bipy molecule in the asymmetric unit. This complex consists of one Cd^{2+} coordinated by four bidentate ligands (two 2,2′-bipy and two acetate). Cadmium is eight-coordinated with a distorted square antiprismatic geometry, where each basal plane is formed by one 2,2′-bipy and one acetate anion (RMSD of 0.191 Å and 0.242 Å for the fitted atoms N1, N2, O3, O4 and N2, N3, O1, O2, respectively). The 2,2′-bipy and acetate ligands comprising a basal plane are almost perpendicular, with the angle between their mean planes of 84.48(17)° and 81.61(17)°. On the other hand, 2,2′-bipy and acetate from different basal planes are not so bent, with an angle between their mean planes of 34.15(14)° and 26.64(16)°.

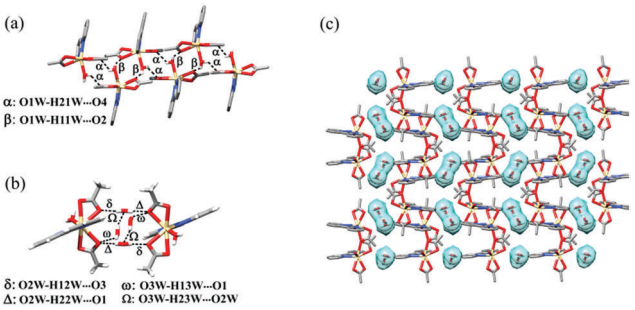

Fig. 10 (a) Infinite chain found in the dihydrate of **2A**. Only hydrogen atoms of coordinated water are shown. (b) Lattice waters bearing O2W and O3W connecting two chains shown in (a) and (c) their arrangement in the overall crystal packing (non-coordinated water molecules are highlighted with cyan surfaces).

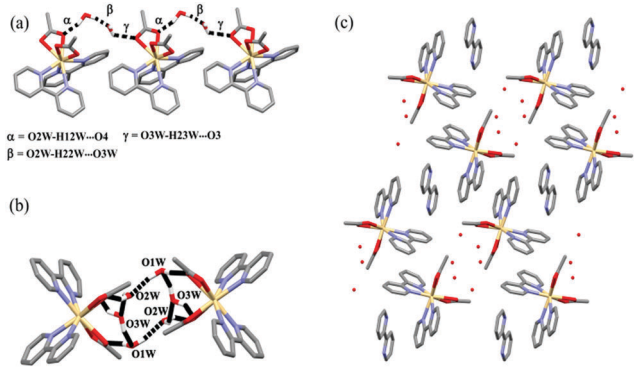

Fig. 11 (a) **2B** molecules are connected by lattice water molecules into the chain formed in its structure. (b) Two neighboring chains connected by O–H···O hydrogen bonds involving non-coordinated water molecules. (c) A packing view of the crystal structure of **2B** showing the cocrystallized 2,2′-bipy molecules between the hydrophobic groups.

Concerning the packing, there is the formation of hydrogen bonded chains alternating **2B** and two non-coordinated water molecules (Fig. 11a). Besides, these water molecules and another crystallographically independent molecule are also responsible for connecting two different chains (Fig. 11b). When viewed along the chain growth direction, it is possible to observe that the complex units are arranged in a head-to-head manner where the hydrophilic motifs and waters are oriented towards each other, while the hydrophobic groups are pointed towards the opposite side relative to the acetate anions and water molecules. Finally, the cocrystallized 2,2′-bipy is held between the tails of complex **2B** through π···π interactions (Fig. 11c).

Crystal structures with Hg^{2+}

The hydrate of 3A: $[Hg(CH_3CO_2)_2(2,2'\text{-bipy})]\cdot(H_2O)$. This structure was solved in the monoclinic space group $P21/c$, with one complex of formula $[Hg(CH_3CO_2)_2(2,2'\text{-bipy})]$ and one crystallizing water molecule in the asymmetric unit. The complex unit consists of Hg^{2+} coordinated by three bidentate ligands (one 2,2′-bipy and two acetate). The complex backbone in this crystal structure resembles those observed for compounds **1B** and **2A**. The Hg^{2+} ion is six-coordinated with a distorted trigonal prismatic geometry, whereas the triangular faces of the trigonal prism are defined by two oxygens from two different acetate anions (O2, O3 or O1, O4) and one nitrogen atom (N1 or N2). The largest trigonal twist angle is 13.0(3)° and the triangular faces are parallel to each other making an angle of 4.93(2)°. The 2,2′-bipy and one acetate are not so bent, with angles between their mean planes measuring 36.8(2)°, while the other acetate ligand is almost perpendicular to 2,2′-bipy, with an angle of 78.8(3)° between their mean planes.

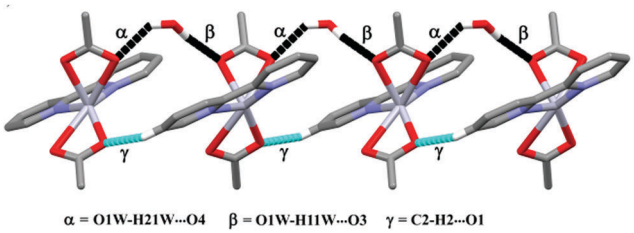

Fig. 12 The chain formed in the crystal packing of **3A**.

The crystal packing of **3A** also features the formation of molecular chains wherein complex units are connected by crystallizing water molecules (Fig. 12). Besides, the other acetate ligand is engaged in non-classical hydrogen bonds C–H···O with the 2,2′-bipy molecule, which assists in the stabilization of such chains (Fig. 12).

The 2,2′-bipy 0.5-cocrystal of the 3B acetate salt octahydrate: $[Hg(CH_3CO_2)(2,2'\text{-bipy})_2](CH_3CO_2)\cdot(2,2'\text{-bipy})_{0.5}\cdot(H_2O)_8$. The persistence of at least one coordinated acetate was found in the new crystal form of the known $[Hg(CH_3CO_2)(2,2'\text{-bipy})_2]^+$ complex, whose previous crystal structure was present with sulfate, chloride and sodium counterions.[25] It is the 2,2′-bipy 0.5-cocrystal of the acetate salt octahydrate obtained under equimolar ligand ratios and even under twice and 10-times 2,2′-bipy excess relative to acetate. This structure shows that 2,2′-bipy can even be cocrystallized in the lattice upon high availability, but no acetate substitution is possible. A similar behavior of such persistence has been reported for mercury(II) trifluoroacetate and 2,2′-bipy ligands.[36] In fact, the removal of all acetate ligands occurred only in Zn^{2+} and Cd^{2+} complexes.

The crystal structure of **3B** was solved in the monoclinic space group $P2_1/c$ and is formed by a discrete cationic complex molecule made up of one Hg^{2+}, one acetate, and two 2,2′-bipy ligands. In this complex, the metal center resides in an octahedral geometry that is defined by the four nitrogen donor atoms of the two 2,2′-bipy ligands, and two oxygens of acetate ligands.

In addition, the asymmetric unit has one half of a 2,2′-bipy molecule, one acetate counterion and eight water molecules. The coordination pattern of complex **3B** bears a resemblance to the structure reported by Ramazani and co-workers,[25] since both 2,2′-bipy molecules and acetate ligands are coordinated to Hg^{2+} in a bidentate manner. The 2,2′-bipy ligands are slightly more bent in our structure than in the known sodium chloride sulfate salt.[25] Here, the angle between the 2,2′-bipy mean planes in complex **3B** is 56.967(10)°, while it measures 68.634(21)° and 73.621(20)° for each crystallographically independent molecule found in the structure reported by Ramazani and coworkers.[25] This occurs due to a rotation about the Hg–N bond axis (Fig. 13). These conformational features can also be observed by looking at the molecule overlay between the complex molecules **3B** found here and those reported earlier.[25] Since the structure reported by Ramazani[25] has two motifs of the cationic complex $[Hg(CH_3CO_2)(2,2'\text{-bipy})_2]^+$ in its asymmetric unit, the calculated RMSD values through the coordinated atoms and metal ions were 0.371 Å and 0.448 Å (Fig. 13).

Unlike the antecedent crystal forms,[25,36] there is cocrystallization of one 2,2′-bipy molecule between two motifs of **3B**. Thus, as

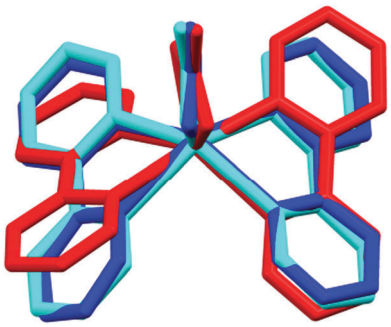

Fig. 13 Molecular overlay of complex **3B** backbones found in our complex (red) and in sodium chloride sulfate salt (two crystallographically independent molecules; light blue centered on Hg1 and blue centered on Hg2).[25]

observed for complex **2B**, this study strengthens the fact that the ligand stoichiometry and reaction conditions are important factors in the process of crystallization of coordination complexes, since on changing their proportions new solid forms can be obtained even if a certain complex molecular structure is retained. Similarly, as it occurs in complexes **1C** and **1D**, this compound also shows the formation of hydrophilic channels within this structure (Fig. 14). Besides water molecules, there are also acetate units filling the channels. In this way, the charge balance is achieved, since complex **3B** is positively charged.

The water molecules within the channels are engaged in a complex hydrogen bonding network, giving rise to an intermolecular ring made up of water molecules bearing O4W, O6W and O7W oxygens (Fig. 14a). The other water molecules are in

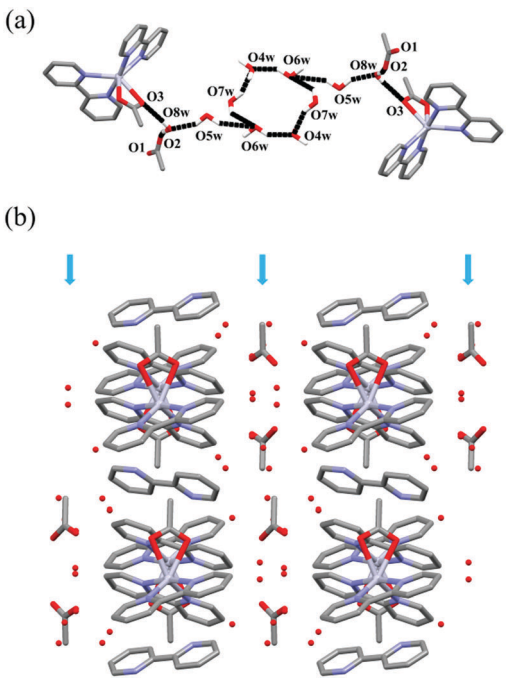

Fig. 14 (a) Molecules of **3B** connected with water molecules within the channels. (b) Layered structure intercalating water and acetate species with molecules of complex **3B** and 2,2′-bipy molecules. The blue arrows indicate the channels filled with water and acetate units.

charge of connecting this water ring and layers of complex **3B** through their hydrogen bonding functionalities. Also, the acetate units help in the stabilization of this mesh of hydrogen bonding (Fig. 14a). Therefore, resembling the structure of **1D**, these sets of hydrogen bonds give rise to a layered structure intercalating the channels, filled with water and acetate units, and the molecules of **3B** and cocrystallized 2,2′-bipy (Fig. 14b).

Photoluminescence emission measurements

In Fig. 15, the photoluminescence (PL) excitation and emission spectra of crystal forms **1C** and **2B** are presented. These are the only crystal forms prepared in this study exhibiting significant PL [internal quantum yield (IQY) higher than 1%]. Even the two Hg^{2+} complexes were extremely weak light-emitting materials whose IQY couldn't be measured even on using wider band passes. Their excitation and emission spectra are shown in the ESI† (Fig. S21 and S22).

The excitation spectrum of **1C** was acquired by monitoring the emission at 356 nm and 448 nm, however the only band with a relevant emission was at 356 nm. Also, emission spectra are shown for excitations at 272, 303, 326 and 380 nm wavelengths. Two bands between 270 and 330 nm are observed in the excitation photoluminescence spectra, which led to a broad band emission between 320 nm and 420 nm (ultraviolet, violet and blue emissions), with the maximum at 356 nm, corresponding to deep-blue colour (colorimetric coordinates $x = 0.179$ and $y = 0.110$; for blue colour $x = 0.17$ and $y = 0.00$). A high external quantum yield (EQY) of 14.2(1)% was observed with a corresponding IQY of 41.3(1)% under excitation at 326 nm. A less efficient PL emission centered at 440 nm was observed for **2B** under excitation at 378 nm, upon emission measurement from 388 nm to 746 nm, EQY and IQY values of 0.7% and 4.1% were found for this light-blue colour emission (colorimetric coordinates $x = 0.170$ and $y = 0.124$).

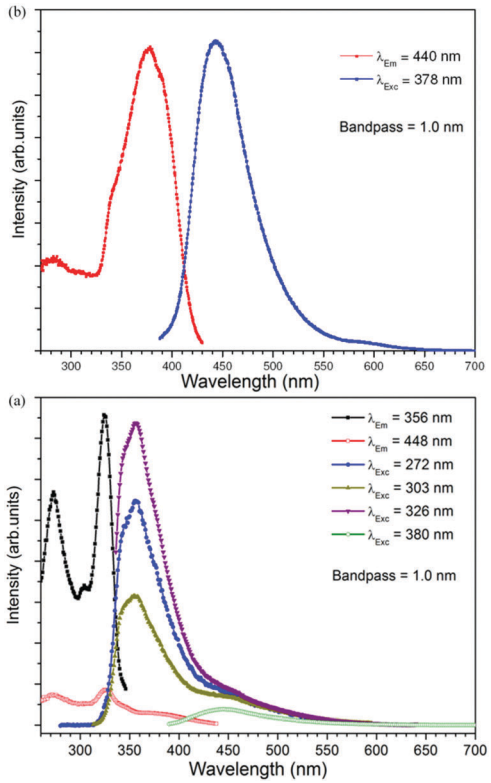

Fig. 15 Photoluminescence excitation and emission spectra of (a) **1C** and (b) **2B** crystals.

Table 1 Time-dependent DFT wavelengths and oscillator strengths for the first ten vertical excitations of **1C**. Transitions with larger oscillator strengths are denoted in bold

Excited state	Main transition (% contribution)	Wavelength	f
S1	HOMO → LUMO (99.7%)	389.09	0.0008
S2	HOMO → LUMO+1 (99.7%)	377.47	0.0016
S3	HOMO−1 → LUMO (99.5%)	340.29	0.0015
S4	HOMO−1 → LUMO+1 (99.0%)	331.62	0.0017
S5	**HOMO−2 → LUMO (97.3%)**	**323.64**	**0.0131**
S6	HOMO−2 → LUMO+1 (97.7%)	316.83	0.0099
S7	HOMO → LUMO+2 (94.7%)	300.8	0.0015
S8	HOMO → LUMO+3 (93.6%)	293.56	0.0002
S9	HOMO → LUMO+4 (96.0%)	281.42	0.0013
S10	**HOMO−3 → LUMO (46.9%)** **HOMO−3 → LUMO+1 (47.7%)**	**279.56**	**0.0716**

To rationalize this efficient optical property of **1C**, we have calculated for **1C** and **2B** the frontier molecular orbitals (FMOs) and the first ten vertical excitations (from S1 to S10) using time-dependent DFT. As can be seen in Fig. S23 and S24 (ESI†), the HOMO and related high-energy occupied FMOs are mainly localized in the acetate ligands, whereas the LUMO and related low-energy unoccupied FMOs are most localized over 2,2′-bipy. A similar trend was observed when using the fully optimized geometries (Fig. S25 and S26, ESI†). In Table 1 and Table S4 (ESI†), the main FMO transitions are shown for **1C** and **2B**, respectively, along with the corresponding wavelengths and oscillator strengths computed using the partially-optimized geometries. It is possible to observe an excellent agreement between the experimental and calculated excitation wavelengths for **1C** with large oscillator strengths (S5 at 323.64 and S10 at 279.56 nm). These theoretical wavelengths are very close to the experimental excitation band centres at 326 nm and 272 nm, rationalizing the high quantum yield of **1C**. Interestingly, the most intense vertical excitation computed from the fully optimized geometry of **1C** (278.2 nm, $f = 0.15$, Table S5, ESI†) was also in good agreement with the experimental values (272 nm). Both transitions at 279.56 nm (partially optimized geometry of **1C**) and 274.5 nm (fully optimized geometry of **1C**) have strong contributions from the HOMO−3 → LUMO and HOMO−3 → LUMO+1 (279.56 nm), and HOMO−3 → LUMO and HOMO−2 → LUMO+1 (278.22 nm) excitations, with these FMOs mainly localized on the 2,2′-bipy system. On the other hand, the oscillator strengths of the first ten excitations of **2B** are negligible, both from the partially and fully optimized geometries (Tables S4 and S6, ESI†).

Conclusions

Herein we have prepared eight new metal-coordination based crystal forms of Zn^{2+}, Cd^{2+} and Hg^{2+} through investigating the competition between 2,2′-bipy and acetate ligands in metal

binding. In addition, two new coordination complexes were synthesized for the first time. It can be concluded that Zn^{2+} reacts better to changes in the ligand proportion, since complexes with 1 : 3, 1 : 2, 2 : 1 and 3 : 0 2,2′-bipy : acetate stoichiometry were formed upon increasing the 2,2′-bipy ratio in the synthesis. Cd^{2+} is less sensible to such changes, but complexes with 1 : 2, 1 : 1, and 3 : 0 2,2′-bipy : acetate stoichiometry were still formed, while only the 1 : 2 and 2 : 1 stoichiometries were found in the Hg^{2+} complexes. Therefore, this study has demonstrated how molecular and structural diversity of coordination complexes can be easily broadened through a simple ligand ratio change, which can be a useful method of getting new functional materials such as the highly efficient photoluminescent crystal form of **1C** obtained here. Furthermore, all syntheses are practical, easy and rapid, requiring only one step, besides presenting low cost and full yield. We believe that the ligand stoichiometric ratio is an attractive approach to conceive new coordination complexes and new crystal forms thereof, which can present desired properties as the efficient PL profile of one of the solid state materials discovered here.

Conflicts of interest

There are no conflicts to declare.

Acknowledgements

The authors acknowledge CNPq, CAPES, and FAPEG for financial support and for research fellowships (JANN, CCS, LJQM and FTM).

Notes and references

1 (*a*) K. Liu, W. Shi and P. Cheng, *Dalton Trans.*, 2011, **40**, 8475–8490; (*b*) D. J. Tranchemontagne, J. L. Mendoza-Cortes, M. O'Keeffe and O. M. Yaghi, *Chem. Soc. Rev.*, 2009, **38**, 1257–1283; (*c*) S. L. James, *Chem. Soc. Rev.*, 2003, **32**, 276–288.
2 R. Chakrabarty, P. S. Mukherjee and P. J. Stang, *Chem. Rev.*, 2011, **111**, 6810–6918.
3 S. Yumi, Y. Sagara, H. Nomura, N. Nakamura, S. Yoshitake, H. Miyazaki and A. Chihaya, *Chem. Commun.*, 2015, **51**, 3181–3184.
4 H. Xu, R. Chen, Q. Sun, W. Lai, Q. Su, W. Huang and X. Liu, *Chem. Soc. Rev.*, 2014, **43**, 3259–3302.
5 T. Sivanandan and S. Kalainathan, *Mater. Chem. Phys.*, 2015, **415**, 25–30.
6 D. Zhao, X.-H. Liu, Z. Shi, C.-D. Zhu, Y. Zhao, P. Wang and W.-Y. Sun, *Dalton Trans.*, 2016, **45**, 14184–14190.
7 Y. Yoshikawa and H. Yasui, *Curr. Top. Med. Chem.*, 2012, **12**, 210–218.
8 B. Zumreoglu-Karan, *Coord. Chem. Rev.*, 2006, **250**, 2295–2307.
9 K. Fujisawa, S. Yamada, Y. Yanagi, Y. Yoshioka, A. Kiyohara and O. Tsutsumi, *Sci. Rep.*, 2015, **5**, 7934–7940.
10 A. Morsali and M. Y. Masoomi, *Coord. Chem. Rev.*, 2009, **253**, 1882–1905.
11 X.-G. Guo, W.-B. Yang, X.-Y. Wu, Q.-K. Zhang, L. Lin, R. Yu and C.-Z. Lu, *CrystEngComm*, 2013, **15**, 3654–3663.
12 P. Kanoo, K. L. Gurunatha and T. K. Maji, *J. Mater. Chem.*, 2010, **20**, 1322–1331.
13 G. Hee, H. Min, M. Young, S. Pyo, C. Kim, J. Ho, S. Joong, S. Kim and Y. Kim, *Polyhedron*, 2011, **30**, 1555–1564.
14 A. Cingolani, S. Galli, N. Masciocchi, L. Pandolfo, C. Pettinari and A. Sironi, *Dalton Trans.*, 2006, 2479–2486.
15 M.-A. Neouze and U. Schubert, *Monatsh. Chem.*, 2008, **139**, 183–195.
16 (*a*) B. H. Ye, X. M. Chen, F. Xue, L. N. Ji and T. C. W. Mak, *Inorg. Chim. Acta*, 2000, **299**, 1–8; (*b*) V. G. Makhankova, O. V. Khavryuchenko, V. V. Lisnyak, V. N. Kokozay, V. V. Dyakonenko, O. V. Shishkin, B. W. Skelton and J. Jezierska, *J. Solid State Chem.*, 2010, **183**, 2695–2702; (*c*) O. V. Nahorna, V. G. Makhankova, V. N. Kokozay, I. V. Omelchenko, V. V. Dyakonenko, O. V. Shishkin and J. Jezierska, *J. Mol. Struct.*, 2013, **1038**, 211–215; (*d*) S. Menage, S. E. Vitols, P. Bergerat, E. Codjovi, O. Kahn, J.-J. Girerd, M. Guillot, X. Solans and T. Calvet, *Inorg. Chem.*, 1991, **30**, 2666–2671.
17 Y. Deng, H. Liu, B. Yu and M. Yao, *Molecules*, 2010, **15**, 3478–3506.
18 J. K. Burdett, C. Marians and J. F. Mitchell, *Inorg. Chem.*, 1994, **33**, 1848–1856.
19 C. Kaes, A. Katz and M. W. Hosseini, *Chem. Rev.*, 2000, **100**, 3553–3590.
20 (*a*) B. L. Rodrigues, *Acta Crystallogr., Sect. E: Struct. Rep. Online*, 2004, **60**, m1169–m1171; (*b*) Z. M. Wang, B. W. Sun, J. Luo, S. Gao, C. S. Liao, C. H. Yan and Y. Li, *Polyhedron*, 2003, **22**, 433–439; (*c*) X. M. Chen, Z.-T. Xu and T. C. W. Mak, *Polyhedron*, 1994, **13**, 3329–3332; (*d*) Z. Talaei, A. Morsali and A. R. Mahjoub, *J. Coord. Chem.*, 2006, **59**, 643–650; (*e*) T. A. Hudson and R. Robson, *Cryst. Growth Des.*, 2009, **9**, 1658–1662.
21 (*a*) J. Breu, H. Domel and A. Stoll, *Eur. J. Inorg. Chem.*, 2000, 2401–2408; (*b*) X. Chen, R.-Q. Wang and X.-L. Yu, *Acta Crystallogr., Sect. C: Cryst. Struct. Commun.*, 1995, **C51**, 1545–1547; (*c*) G. Hee, H. Min, M. Young, S. Pyo, C. Kim, J. Ho, S. Joong, S. Kim and Y. Kim, *Polyhedron*, 2011, **30**, 1555–1564; (*d*) A. Wojciechowska, Z. Staszak, W. Bronowska, A. Pietraszko and M. Cieslak-Golonka, *Polyhedron*, 2001, **20**, 2063–2072.
22 I. S. Ahuja, C. L. Yadava and R. Singh, *Indian J. Chem., Sect. A: Inorg., Phys., Theor. Anal.*, 1981, **20**, 1127–1130.
23 W. Zhang, Z. Jiang and L. Lu, *Acta Crystallogr., Sect. E: Struct. Rep. Online*, 2009, **E65**, m7.
24 T. S. A. Hor, Y. Quah and J. O. Hill, *Proc. Natl. Symp. Therm. Anal., 8th*, 1991, **8**, 141–145.
25 A. Ramazani, G. Mahmoudi, L. Dolatyari, A. Morsali and M.-L. Hu, *J. Coord. Chem.*, 2007, **60**, 2115–2120.
26 *SADABS, APEX2 and SAINT*, Bruker AXS Inc., Madison, Wisconsin, USA, 2009.
27 G. M. Sheldrick, *Acta Crystallogr. Sect. A*, 2008, **64**, 112–122.
28 C. F. Macrae, I. J. Bruno, J. A. Chisholm, P. R. Edgington, P. McCabe, E. Pidcock, L. Rodriguez-Monge, R. Taylor, J. Van De Streek and P. A. Wood, *J. Appl. Crystallogr.*, 2008, **41**, 466–470.

29 L. J. Farrugia, *J. Appl. Crystallogr.*, 2012, **45**, 849–854.
30 P. Hohenberg and W. Kohn, *Phys. Rev.*, 1964, **136**, B864–B871.
31 W. Kohn and L. J. Sham, *Phys. Rev.*, 1965, **140**, A1133–A1138.
32 A. D. Becke, *J. Chem. Phys.*, 1993, **98**, 5648–5652.
33 C. Lee, W. Yang and R. G. Parr, *Phys. Rev. B*, 1988, **37**, 785–789.
34 P. J. Hay and W. R. Wadt, *J. Chem. Phys.*, 1985, **82**, 299–310.
35 M. J. Frisch, G. W. Trucks, H. B. Schlegel, G. E. Scuseria, M. A. Robb, J. R. Cheeseman, G. Scalmani, V. Barone, B. Mennucci, G. A. Petersson, H. Nakatsuji, M. Caricato, X. Li, H. P. Hratchian, A. F. Izmaylov, J. Bloino, G. Zheng, J. L. Sonnenberg, M. Hada, M. Ehara, K. Toyota, R. Fukuda, J. Hasegawa, M. Ishida, T. Nakajima, Y. Honda, O. Kitao, H. Nakai, T. Vreven, J. A. Montgomery Jr., J. E. Peralta, F. Ogliaro, M. Bearpark, J. J. Heyd, E. Brothers, K. N. Kudin, V. N. Staroverov, R. Kobayashi, J. Normand, K. Raghavachari, A. Rendell, J. C. Burant, S. S. Iyengar, J. Tomasi, M. Cossi, N. Rega, J. M. Millam, M. Klene, J. E. Knox, J. B. Cross, V. Bakken, C. Adamo, J. Jaramillo, R. Gomperts, R. E. Stratmann, O. Yazyev, A. J. Austin, R. Cammi, C. Pomelli, J. W. Ochterski, R. L. Martin, K. Morokuma, V. G. Zakrzewski, G. A. Voth, P. Salvador, J. J. Dannenberg, S. Dapprich, A. D. Daniels, O. Farkas, J. B. Foresman, J. V. Ortiz, J. Cioslowski and D. J. Fox, *Gaussian 09*, Gaussian Inc., Wallingford CT, 2009.
36 J. Halfpenny and R. W. H. Small, *Acta Crystallogr. Sect. C*, 1997, **C53**, 438–443.